

## NANO EXPRESS

## Open Access

# Size-regulated group separation of $\text{CoFe}_2\text{O}_4$ nanoparticles using centrifuge and their magnetic resonance contrast properties

Jongeun Kang<sup>1,2</sup>, Hyunseung Lee<sup>1</sup>, Young-Nam Kim<sup>1</sup>, Areum Yeom<sup>1</sup>, Heejeong Jeong<sup>1</sup>, Yong Taik Lim<sup>2</sup> and Kwan Soo Hong<sup>1,2\*</sup>

## Abstract

Magnetic nanoparticle (MNP)-based magnetic resonance imaging (MRI) contrast agents (CAs) have been the subject of extensive research over recent decades. The particle size of MNPs varies widely and is known to influence their physicochemical and pharmacokinetic properties. There are two commonly used methods for synthesizing MNPs, organometallic and aqueous solution coprecipitation. The former has the advantage of being able to control the particle size more effectively; however, the resulting particles require a hydrophilic coating in order to be rendered water soluble. The MNPs produced using the latter method are intrinsically water soluble, but they have a relatively wide particle size distribution. Size-controlled water-soluble MNPs have great potential as MRI CAs and in cell sorting and labeling applications. In the present study, we synthesized  $\text{CoFe}_2\text{O}_4$  MNPs using an aqueous solution coprecipitation method. The MNPs were subsequently separated into four groups depending on size, by the use of centrifugation at different speeds. The crystal shapes and size distributions of the particles in the four groups were measured and confirmed by transmission electron microscopy and dynamic light scattering. Using X-ray diffraction analysis, the MNPs were found to have an inverse spinel structure. Four MNP groups with well-selected semi-Gaussian-like diameter distributions were obtained, with measured  $T_2$  relaxivities ( $r_2$ ) at 4.7 T and room temperature in the range of 60 to 300  $\text{mM}^{-1}\text{s}^{-1}$ , depending on the particle size. This size regulation method has great promise for applications that require homogeneous-sized MNPs made by an aqueous solution coprecipitation method. Any group of the  $\text{CoFe}_2\text{O}_4$  MNPs could be used as initial base cores of MRI  $T_2$  CAs, with almost unique  $T_2$  relaxivity owing to size regulation. The methodology reported here opens up many possibilities for biosensing applications and disease diagnosis.

**Keywords:** Magnetic nanoparticles; Magnetic resonance imaging; Relaxivity; Particle size regulation

**PACS:** 75.75.Fk, 78.67.Bf, 61.46.Df

## Background

Magnetic resonance imaging (MRI) is a powerful diagnostic modality for noninvasive *in vivo* imaging due to its high resolution, lack of exposure to radiation, superior soft tissue contrast, and large image window. However, it has less sensitivity than nuclear medicine and fluorescence imaging when monitoring small tissue lesions and molecular or cellular activities [1]. Contrast agents (CAs) can improve the contrast and specificity in particular target regions of MR

images, and these are widely used to produce brighter and darker areas with  $T_1$  and  $T_2$  CAs, respectively.  $T_2$  CAs, mainly based on iron oxide magnetic nanoparticles (MNPs), provide dark contrast in  $T_2$ - or  $T_2^*$ -weighted ( $T_2^*$ -W) MR images depending on the  $T_2$  relaxivity of  $r_2$  and the MNP concentration in the region of interest [2]. Superparamagnetic iron oxide (SPIO) nanoparticles with diameters of 50 to 150 nm are thus the most commonly used MNPs in a variety of biomedical applications such as MRI contrast agents, induction of local hyperthermia, manipulation of cell membranes, biosensors, cell labeling and tracking, and drug targeting and delivery [3-8].

SPIO particles have different physicochemical and biological properties, depending on the particle size and

\* Correspondence: [kshong@kbsi.re.kr](mailto:kshong@kbsi.re.kr)

<sup>1</sup>Center for MR Research, Korea Basic Science Institute, Cheongwon 363-883, South Korea

<sup>2</sup>Graduate School of Analytical Science and Technology, Chungnam National University, Daejeon 305-764, South Korea

coating material, including MR  $T_2$  relaxivity  $r_2$  [9], cell labeling efficiency [10], cell cytotoxicity [11], and *in vivo* pharmacokinetics such as blood half-life and biodistribution [12]. Therefore, strategies by which uniform-sized biocompatible MNPs with long circulation times can be produced are highly sought after for nanomedical applications.

There are two commonly used methods for synthesizing MNPs, organometallic [13] and aqueous solution coprecipitation [14]. In the organometallic approach, the particle size can be easily controlled [15]; however, the MNPs are only soluble in nonpolar and moderately polar organic solvents. This brings about the requirement for hydrophilic and biocompatible polymer coating to make them soluble enough for *in vivo* uses [16-18]. On the other hand, the aqueous solution coprecipitation method results in nanoparticles that are intrinsically water-soluble; however, the particle size distribution is relatively wide, resulting in nonuniform contrast in  $T_2$ - or  $T_2^*$ -W MR images. Size-controlled water-soluble nanoparticles provide the possibility to achieve uniform functionalization of their surfaces with other imaging probes such as fluorescent dyes and radiolabeled probes or with targeting molecules such as antibodies, peptides, and genes, as well as therapeutics [18,19]. Several reports are available regarding the size regulation of MNPs synthesized by coprecipitation, including a temperature-controlled coprecipitation method that requires specialized equipment and a piezoelectric nozzle method [20,21]. These processes are either highly complex or relatively ineffective owing to the requirement for a high level of control over parameters such as temperature during the synthesis. In addition, the produced particles still have an inadequate size distribution. The piezoelectric nozzle method is more effective for controlling the size; however, this technique requires specialized equipment such as a piezoelectric transducer and a frequency amplifier.

To address these issues, a facile method for controlling the MNP core size via the coprecipitation process is introduced here. Initially, we synthesized  $\text{CoFe}_2\text{O}_4$  nanoparticles using an aqueous solution coprecipitation method and then separated the particles into four groups depending on their size by employing a variety of centrifugation speeds. The physicochemical properties of the four groups were subsequently evaluated. The size distribution was assessed by transmission electron microscopy (TEM) and dynamic light scattering (DLS), crystallographic confirmation was carried out by X-ray diffraction (XRD), the water proton  $T_2$  relaxation rate ( $R_2$ ) versus Co/Fe concentration was evaluated, and MR image contrast was measured at 4.7 T.

## Methods

### Synthesis of $\text{CoFe}_2\text{O}_4$ nanoparticles

The  $\text{CoFe}_2\text{O}_4$  MNPs were synthesized by an aqueous solution coprecipitation method reported previously [14].

Initially, the reagents, 0.5 M  $\text{FeCl}_3 \cdot 6\text{H}_2\text{O}$  ( $\geq 98\%$ ; Sigma-Aldrich, Tokyo, Japan) and 0.25 M  $\text{CoCl}_2 \cdot 6\text{H}_2\text{O}$  (99% to 102%; Sigma-Aldrich), were mixed in an aqueous solution, giving a Co/Fe ratio of 1:2. The reaction mixture was stirred vigorously for 6 h in boiling distilled water with 1 M NaOH (96%; Junsei, Tokyo, Japan), and then, the resulting dark brown suspension was centrifuged at  $1,771 \times g$ . The precipitate was dissolved in a 2-M  $\text{HNO}_3$  solution with stirring for 20 min and then centrifuged again at  $1,771 \times g$ . The resulting precipitate was dissolved in 0.5 M  $\text{Fe}(\text{NO}_3)_3$  ( $\geq 98\%$ ; Sigma-Aldrich) and stirred vigorously for 30 min at  $100^\circ\text{C}$ . After the reaction, centrifugation at  $1,771 \times g$  and redispersion in distilled water were performed three times. Finally, the suspension was dissolved in water and stored at room temperature until further use.

### Size selection of MNPs and synthesis of $\text{SiO}_2$ -coated MNPs

As the synthesized MNPs had a broad size distribution between 5 and 300 nm, they were separated depending on their size by stepwise centrifugation. A high-speed vacuum centrifuge system was used (SUPRA 25K; Hanil Scimed, Gangneung, Korea), with five different speeds of  $1,771 \times g$ ,  $2,767 \times g$ ,  $11,068 \times g$ ,  $24,903 \times g$ , and  $35,860 \times g$  in order to separate the synthesized particles into four groups. Firstly, aggregated particles were removed by down-sinking with  $1,771 \times g$  for 1 h. The remaining mixture was centrifuged at  $35,860 \times g$  for 1 h, and then, the suspended solution was removed. Resuspension of the bottom layer provided the initial MNP solution. This was then centrifuged at  $2,767 \times g$ ,  $11,068 \times g$ , and  $24,903 \times g$  for 1 h, with the bottom layer collected as groups A, B, and C, respectively. The first suspended solution remaining after centrifugation at  $24,903 \times g$  was labeled as group D. The MNPs of group C were selected for  $\text{SiO}_2$  coating for further applications.  $\text{SiO}_2$  coating was done as follows: the MNPs of group C were stabilized with polyvinylpyrrolidone (PVP) to disperse them homogeneously, and then, tetraethoxysilane solution was polymerized on the surface of PVP-stabilized  $\text{CoFe}_2\text{O}_4$  MNPs by adding ammonia solution as a catalyst to form  $\text{SiO}_2$  coating on the MNPs. The volume ratio of the ammonia solution was 4.2% to control the  $\text{SiO}_2$  shell thickness of the final  $\text{SiO}_2$ -coated MNPs in this process.

### MNP characterization

The crystal shapes and structures of the synthesized MNPs in each group, in addition to the  $\text{SiO}_2$ -coated MNPs, were measured and confirmed by TEM (Tecnai G2 F30, FEI, Hillsboro, OR, USA) and XRD (XPERT MPD, Philips, Amsterdam, The Netherlands). The XRD patterns were compared with a typical XRD spectrum of a  $\text{CoFe}_2\text{O}_4$  crystal. The hydrodynamic diameter distribution of the particles was measured by DLS (UPA-150I, Microtrac, Montgomeryville, PA, USA), and the size distribution was verified from the TEM images.

In order to compare  $T_2$  relaxivities ( $r_2$ ) of the four groups and the  $\text{SiO}_2$ -coated MNPs, the  $T_2$  relaxation times were measured against the Co/Fe concentration in a range below 1 mM Fe using a spin-echo pulse sequence (multi-spin multi-echo) on a 4.7-T animal MRI system (Biospec 47/40; Bruker, Karlsruhe, Germany). The amount of Co/Fe in each group was measured using an inductively coupled plasma atomic emission spectrometry system (Optima 4300DV, PerkinElmer, Waltham, MA, USA). For the MRI experiment, the MNPs were sampled at four different Co/Fe concentrations of 1.0, 0.75, 0.5, and 0.25 mM Co/Fe in distilled water in 250- $\mu\text{l}$  microtubes. The MRI parameters used were as follows: TE/TR = 10/10,000 ms, number of scans = 2, slice thickness = 1 mm, FOV =  $5 \times 5 \text{ cm}^2$ , number of slices = 1.  $T_2$  contrast differences depending on Fe concentration for the separated groups were also compared in  $T_2$ -W MR images.

## Results and discussion

The MNPs synthesized by the coprecipitation method were found to have an extremely broad size distribution [14]. This characteristic would likely result in nonuniform contrast in MR images. The purpose of the present study was to overcome this limitation by separating the different sizes of particles by centrifugation. After the initial removal of

aggregates, the nanoparticles were sequentially centrifuged at speeds  $2,767 \times g$ ,  $11,068 \times g$ ,  $24,903 \times g$ , and  $35,860 \times g$ , producing groups A, B, C, and D, respectively. As shown in the TEM images in Figure 1, the centrifugation process resulted in four groups containing particles relatively uniform in size. The mean diameters measured from approximately 100 randomly selected particles from each group were found to be  $24.2 \pm 3.6$ ,  $20.0 \pm 3.6$ ,  $15.8 \pm 3.6$ , and  $10.5 \pm 2.4$  nm for groups A, B, C, and D, respectively. As the rotational speed increased, the MNP diameters decreased, with significant differences between adjacent groups ( $P < 0.01$ ). The hydrodynamic diameter distributions of the MNPs in the four groups were Gaussian-like, with values of  $65.5 \pm 14.0$ ,  $38.9 \pm 9.1$ ,  $23.1 \pm 6.0$ , and  $18.5 \pm 4.4$  nm (Figure 2a) and volume ratios of 29%, 48%, 13%, and 10% for groups A to D, respectively. Further, from the measured volume ratios in Figure 2a, the highest MNP volume was observed for group B; groups C and D could also provide an adequate quantity of uniform-sized MNPs for use in applications that require very small sized (approximately 10 nm) MNPs. The amount of synthesized MNPs from group D was approximately 0.5 g, which could be easily scaled-up using a larger reaction vessel.

The mean diameter of the MNPs, as measured by TEM and DLS, decreased as the centrifugation speed

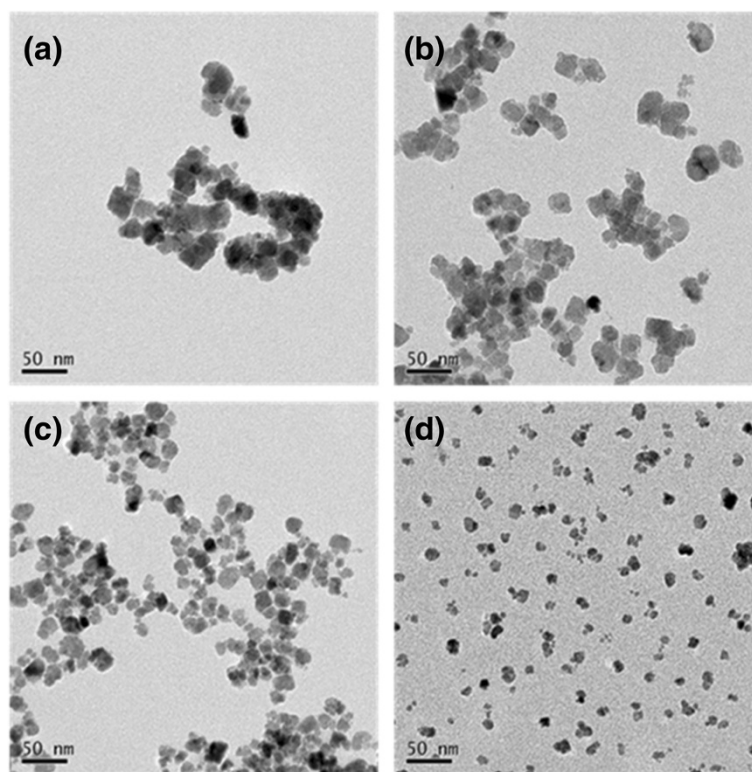
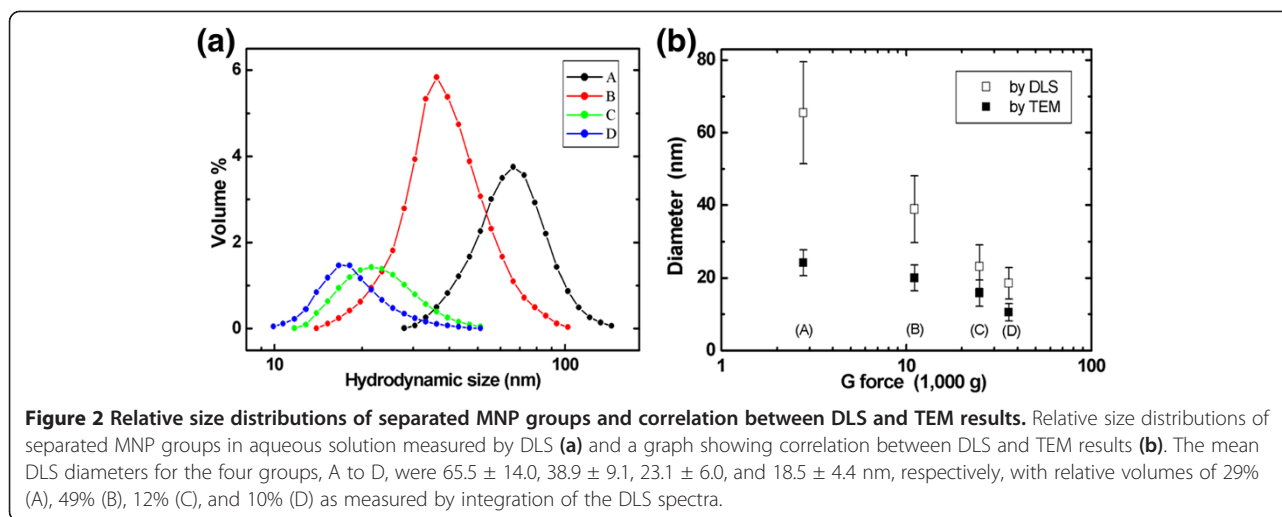


**Figure 1** TEM images of the four MNP groups. The TEM images show that the particles were well dispersed and size-regulated according to the group. The mean diameters for the four groups were  $24.2 \pm 3.6$ ,  $20.0 \pm 3.6$ ,  $15.8 \pm 3.6$ , and  $10.5 \pm 2.4$  nm, for groups **a** to **d**, respectively.

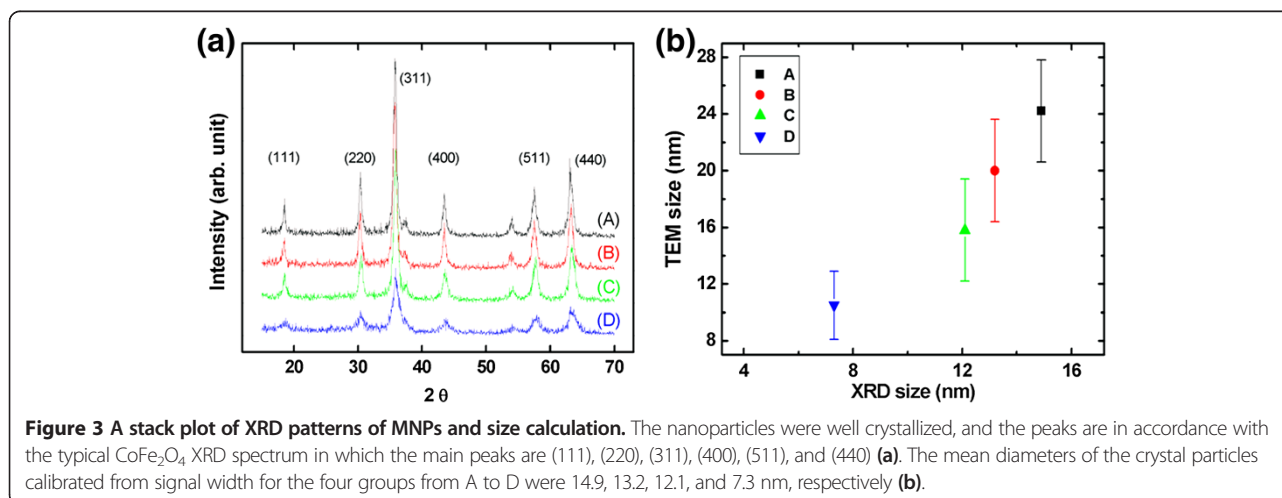


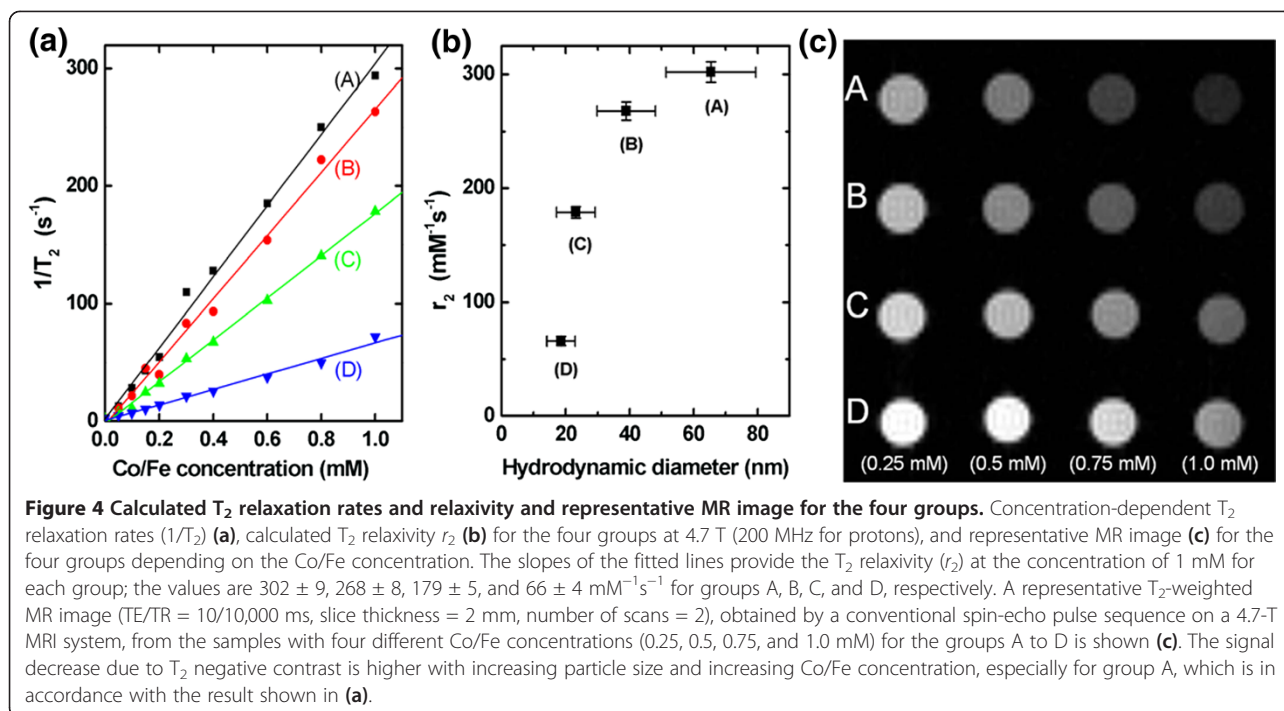
decreased (Figure 2b), indicating that the MNP particles synthesized by the coprecipitation method were well separated and clearly resolved into the four groups by the different centrifugation speeds.

Using the organometallic method reported by others, the particle size of MNPs can be easily controlled, with a narrower diameter distribution achievable in comparison to the combined coprecipitation and centrifugation methods described here. However, the amount of MNPs that can be synthesized in a single process is quite small, and these have the added disadvantage of being hydrophobic. A coating is therefore necessary in order to render these MNPs hydrophilic and to enable them to be used for functions such as drug loading, targeting, or imaging probes (PET or fluorescence). Even though the size distribution of MNPs synthesized by the coprecipitation method was large, huge amounts of size-controlled MNPs were obtained by combining the method with a

simple centrifugation process. Figure 3a shows the XRD results obtained for the four groups of  $\text{CoFe}_2\text{O}_4$  MNPs. All groups can be seen to exhibit the same peaks, which match well with the standard  $\text{Fe}_3\text{O}_4$  XRD pattern (JCPDS 75–0030). The mean particle size ( $D$ ) can be calculated by the full-width at half-maximum (FWHM) and the area/height ratio ( $\beta$ ) of the XRD peaks with instrumental correction, using the equation  $D = K\lambda / \beta \times \cos\theta$ , where  $K$  is the Scherrer constant,  $\lambda$  is the wavelength,  $\beta$  is the FWHM (in radians), and  $\theta$  is the peak angular position [22,23]. The XRD information gave crystallite sizes of 14.9, 13.2, 12.1, and 7.3 nm (Figure 3). As MNPs synthesized by coprecipitation may contain some iron oxide crystals, the particle size calculated from the TEM images was larger than that from the XRD data (Figure 3b).

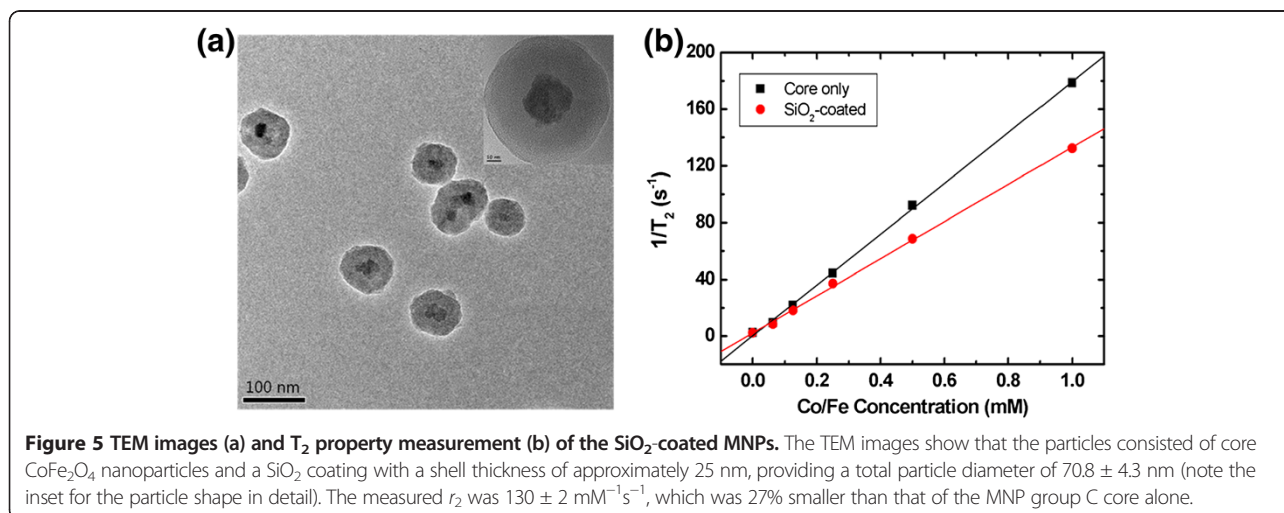
The size-dependent MR contrast ( $T_2$  relaxivity) of the MNPs was measured on a 4.7-T MRI system. Figure 4a shows the dependence of the  $T_2$  relaxation rate ( $R_2, \text{s}^{-1}$ )





on the MNPs of the four groups. The  $T_2$  relaxation rate was increased with increased Co/Fe concentration, and the  $T_2$  relaxivities ( $r_2$ ) for the groups were measured from the slopes of the data. The  $r_2$  values were found to be  $302 \pm 9$ ,  $268 \pm 8$ ,  $179 \pm 5$ , and  $66 \pm 4$   $\text{mM}^{-1}\text{s}^{-1}$  for groups A, B, C, and D, respectively (Figure 4b). These values are comparable to those in the study of Joshi et al. [24], in which the  $T_2$  relaxivity of cobalt ferrite nanostructures synthesized by the thermal decomposition method was reported to be 110 to 301  $\text{mM}^{-1}\text{s}^{-1}$  depending on the particle size (6 to 15 nm). Figure 4c shows an MRI phantom image with the four groups depending on the

Co/Fe concentration measured on the 4.7-T MRI system. The increase in MR  $T_2$  negative contrast was shown to depend on both the particle diameter and the Co/Fe concentration, indicating that a well-controlled contrast with each size-selected group of MNPs could be obtained. The particle size dependence of  $T_2$  relaxivity was in accordance with other reports [25,26], in which  $T_2$  spin-spin relaxation is affected by mass magnetization depending on the magnetic particle size in the range lower than approximately 1  $\mu\text{m}$ . This demonstrates that each group of MNPs could be used for specific applications depending on the particle diameter. One concern regarding these as-prepared MNPs



is that they are not stable to variations in pH. This is a problem that needs to be overcome if they are to be successfully employed *in vivo*. We therefore investigated the coating of the MNPs with a stable and biocompatible material such as SiO<sub>2</sub> to enhance stability and avoid potential toxic effects on cells (Figure 5) [19]. The T<sub>2</sub> relaxivity of the SiO<sub>2</sub>-coated MNPs made from group C was 130 ± 2 mM<sup>-1</sup>s<sup>-1</sup> (Figure 5b), which was approximately 27% lower than that of the original core particles. Group C was selected for SiO<sub>2</sub> coating in order to get final SiO<sub>2</sub>-coated SPIO MNPs with a diameter of 50 to 100 nm and with a moderate T<sub>2</sub> relaxivity value. The SiO<sub>2</sub> coating would facilitate the addition of therapeutic and targeting functions such as drugs and antibodies to the MNPs, enabling them to serve as both imaging agents and a therapeutic carrier species.

There have been several reports on Fe<sub>3</sub>O<sub>4</sub>-based MNPs with a narrow size distribution made by the coprecipitation method. Lee et al. used a piezoelectric nozzle [20], which, despite effectively controlling the particle size, requires specialized equipment and many steps. Jiang et al. employed a coprecipitation methodology using urea, which provided SPIO MNPs with a narrow size distribution [27]. The average diameter of these MNPs could be adjusted from 8 to 50 nm depending on the decomposition of urea in the ferrite solution; however, they required additional dextran coating in order to make them water soluble. In the present study, the use of centrifugation in combination with the coprecipitation method enabled effective regulation of the size of the MNPs without the requirement for a specialist. A large quantity of each size of particles could be produced, overcoming many of the shortcomings of the coprecipitation method.

## Conclusions

A simple centrifugation technique was combined with a coprecipitation method in aqueous solution in order to obtain four groups of CoFe<sub>2</sub>O<sub>4</sub> MNPs. These were successfully produced in large quantities, with different diameters and MRI T<sub>2</sub> relaxivity values and narrow size distributions, depending on the centrifugation speed. The obtained MNPs had a strong size-dependent MRI T<sub>2</sub> contrast with T<sub>2</sub> relaxivities between 302 and 66 mM<sup>-1</sup>s<sup>-1</sup>, providing a selection of particles from which the most appropriate for a specific application could be chosen. In the present study, the particles of group C were selected for additional SiO<sub>2</sub> coating. This was to demonstrate the potential of these MNPs to be used for *in vivo* applications where they would require a long blood half-life, in addition to biocompatibility. Each of the groups of CoFe<sub>2</sub>O<sub>4</sub> MNPs could be used as the initial base cores of MRI T<sub>2</sub> contrast agents, with almost unique T<sub>2</sub> relaxivity due to the size regulation. This opens up many possibilities for biosensing applications and disease diagnosis.

## Abbreviations

CAs: Contrast agents; DLS: Dynamic light scattering; FWHM: Full-width at half-maximum; MNP: Magnetic nanoparticle; MRI: Magnetic resonance imaging; SPIO: Superparamagnetic iron oxide; TEM: Transmission electron microscopy; XRD: X-ray diffraction.

## Competing interests

The authors declare that they have no competing interests.

## Authors' contributions

JK, YTL, and KSH designed the experiments. JK, HL, AY, and Y-NK performed the experiments. JK, Y-NK, and HJ analyzed the data. JK, HL, AY, and HJ made the figures. JK and KSH wrote the manuscript. All authors read and approved the final manuscript.

## Acknowledgements

This work was supported by grants from the Korean Ministry of Education, Science and Technology (2011-0029263); the Korea Health Technology R&D Project, Ministry of Health and Welfare (A111499); and the CAP (PBC066) funded by the Korea Research Council of Fundamental Science and Technology (KRCF).

Received: 23 June 2013 Accepted: 23 August 2013

Published: 3 September 2013

## References

1. Judenhofer MS, Wehrl HF, Newport DF, Catana C, Siegel SB, Becker M, Thielscher A, Kneilling M, Lichy MP, Eichner M, Klingel K, Reischl G, Widmaier S, Rocken M, Nutt RE, Machulla HJ, Uludag K, Cherry SR, Claussen CD, Pichler BJ: **Simultaneous PET-MRI: a new approach for functional and morphological imaging.** *Nat Med* 2008, **14**:459–465.
2. Lu AH, Salabas EL, Schuth F: **Magnetic nanoparticles: synthesis, protection, functionalization, and application.** *Angew Chem Int Ed Engl* 2007, **46**:1222–1244.
3. Tanaka K, Narita A, Kitamura N, Uchiyama W, Morita M, Inubushi T, Chujo Y: **Preparation for highly sensitive MRI contrast agents using core/shell type nanoparticles consisting of multiple SPIO cores with thin silica coating.** *Langmuir* 2010, **26**:11759–11762.
4. Artan Y, Haider MA, Langer DL, van der Kwast TH, Evans AJ, Yang Y, Wernick MN, Trachtenberg J, Yetik IS: **Prostate cancer localization with multispectral MRI using cost-sensitive support vector machines and conditional random fields.** *IEEE Trans Image Process* 2010, **19**:2444–2455.
5. Bennewitz MF, Lobo TL, Nkansah MK, Ulas G, Brudvig GW, Shapiro EM: **Biocompatible and pH-sensitive PLGA encapsulated MnO nanocrystals for molecular and cellular MRI.** *ACS Nano* 2011, **5**:3438–3446.
6. Chertok B, Moffat BA, David AE, Yu F, Bergemann C, Ross BD, Yang VC: **Iron oxide nanoparticles as a drug delivery vehicle for MRI monitored magnetic targeting of brain tumors.** *Biomaterials* 2008, **29**:487–496.
7. Branca RT, Cleveland ZI, Fubara B, Kumar CS, Maronpot RR, Leuschner C, Warren WS, Driehuys B: **Molecular MRI for sensitive and specific detection of lung metastases.** *Proc Natl Acad Sci USA* 2010, **107**:3693–3697.
8. Sonvico F, Mornet S, Vasseur S, Dubernet C, Jaillard D, Degrouard J, Hoebeke J, Duguet E, Colombo P, Couvreur P: **Folate-conjugated iron oxide nanoparticles for solid tumor targeting as potential specific magnetic hyperthermia mediators: synthesis, physicochemical characterization, and *in vitro* experiments.** *Bioconjug Chem* 2005, **16**:1181–1188.
9. Tromsdorf UI, Bigall NC, Kaul MG, Bruns OT, Nikolic MS, Mollwitz B, Sperling RA, Reimer R, Hohenberg H, Parak WJ, Forster S, Beisiegel U, Adam G, Weller H: **Size and surface effects on the MRI relaxivity of manganese ferrite nanoparticle contrast agents.** *Nano Lett* 2007, **7**:2422–2427.
10. Thorek DL, Tsourkas A: **Size, charge and concentration dependent uptake of iron oxide particles by non-phagocytic cells.** *Biomaterials* 2008, **29**:3583–3590.
11. Matuszewski L, Persigehl T, Wall A, Schwindt W, Tombach B, Fobker M, Poremba C, Ebert W, Heindel W, Bremer C: **Cell tagging with clinically approved iron oxides: feasibility and effect of lipofection, particle size, and surface coating on labeling efficiency.** *Radiology* 2005, **235**:155–161.
12. Chouly C, Pouliquen D, Lucet I, Jeune JJ, Jallet P: **Development of superparamagnetic nanoparticles for MRI: effect of particle size, charge and surface nature on biodistribution.** *J Microencapsul* 1996, **13**:245–255.

13. Yu WW, Falkner JC, Yavuz CT, Colvin VL: **Synthesis of monodisperse iron oxide nanocrystals by thermal decomposition of iron carboxylate salts.** *Chem Commun* 2004, **0**:2306–2307.
14. Hasegawa KR, Saw T: **Particle-size distribution of CoFe<sub>2</sub>O<sub>4</sub> formed by the coprecipitation method.** *J Appl Phys* 1967, **38**:4707–4712.
15. Jana NR, Chen Y, Peng X: **Size- and shape-controlled magnetic (Cr, Mn, Fe, Co, Ni) oxide nanocrystals via a simple and general approach.** *Chem Mater* 2004, **16**:3931–3935.
16. Lee HY, Lee SH, Xu C, Xie J, Lee JH, Wu B, Koh AL, Wang X, Sinclair R, Wang SX, Nishimura DG, Biswal S, Sun S, Cho SH, Chen X: **Synthesis and characterization of PVP-coated large core iron oxide nanoparticles as an MRI contrast agent.** *Nanotechnology* 2008, **19**:165101–165106.
17. Mulder WJ, Strijkers GJ, van Tilborg GA, Griffioen AW, Nicolay K: **Lipid-based nanoparticles for contrast-enhanced MRI and molecular imaging.** *NMR Biomed* 2006, **19**:142–164.
18. Laurent S, Forge D, Port M, Roch A, Robic C, van der Elst L, Muller RN: **Magnetic iron oxide nanoparticles: synthesis, stabilization, vectorization, physicochemical characterizations, and biological applications.** *Chem Rev* 2008, **108**:2064–2110.
19. Yoon TJ, Yu KN, Kim E, Kim JS, Kim BG, Yun SH, Sohn BH, Cho MH, Lee JK, Park SB: **Specific targeting, cell sorting, and bioimaging with smart magnetic silica core-shell nanomaterials.** *Small* 2006, **2**:209–215.
20. Lee SJ, Jeong JR, Shin SC, Kim JC, Kim JD: **Synthesis and characterization of superparamagnetic maghemite nanoparticles prepared by coprecipitation technique.** *J Magn Magn Mater* 2004, **282**:147–150.
21. Kim YI, Kim D, Lee CS: **Synthesis and characterization of CoFe<sub>2</sub>O<sub>4</sub> magnetic nanoparticles prepared by temperature-controlled coprecipitation method.** *Physica B* 2003, **337**:42–53.
22. Ibrahim MM, Zhao J, Seehra MS: **Determination of particle size distribution in an Fe<sub>2</sub>O<sub>3</sub>-based catalyst using magnetometry and X-ray diffraction.** *J Mater Res* 1992, **7**:1856–1860.
23. Crosa M, Boero V, Angela MF: **Determination of mean crystallite dimensions from X-ray diffraction peak profiles: a comparative analysis of synthetic hematites.** *Clays Clay Miner* 1999, **47**:742–747.
24. Joshi HM, Lin YP, Aslam M, Prasad PV, Schultz-Sikma EA, Edelman R, Meade T, Dravid VP: **Effects of shape and size of cobalt ferrite nanostructures on their MRI contrast and thermal activation.** *J Phys Chem C* 2009, **113**:17761–17767.
25. Jun Y, Huh YM, Choi J, Lee JH, Song HT, Kim S, Yoon S, Kim KS, Shin JS, Suh JS, Cheon J: **Nanoscale size effect of magnetic nanocrystals and their utilization for cancer diagnosis via magnetic resonance imaging.** *J Am Chem Soc* 2005, **127**:5732–5733.
26. Shapiro EM, Skrtic S, Sharer K, Hill JM, Dunbar CE, Koretsky AP: **MRI detection of single particles for cellular imaging.** *Proc Natl Acad Sci USA* 2004, **101**:10901–10906.
27. Jiang W, Yang HC, Yang SY, Horng HE, Hung JC, Chen YC, Hong CY: **Preparation and properties of superparamagnetic nanoparticles with narrow size distribution and biocompatible.** *J Magn Magn Mater* 2004, **283**:210–214.

doi:10.1186/1556-276X-8-376

**Cite this article as:** Kang et al.: Size-regulated group separation of CoFe<sub>2</sub>O<sub>4</sub> nanoparticles using centrifuge and their magnetic resonance contrast properties. *Nanoscale Research Letters* 2013 **8**:376.

**Submit your manuscript to a SpringerOpen<sup>®</sup> journal and benefit from:**

- Convenient online submission
- Rigorous peer review
- Immediate publication on acceptance
- Open access: articles freely available online
- High visibility within the field
- Retaining the copyright to your article

---

Submit your next manuscript at ► [springeropen.com](http://springeropen.com)